Cardiovascular Research (2015) **106**, 131–142
doi:10.1093/cvr/cvv030

miR-30e targets IGF2-regulated osteogenesis in bone marrow-derived mesenchymal stem cells, aortic smooth muscle cells, and ApoE$^{-/-}$ mice

Wen Ding[1,2], Jihe Li[2,3], Jayanti Singh[2,3], Razan Alif[4], Roberto I. Vazquez-Padron[5,6], Samirah A. Gomes[2], Joshua M. Hare[2,3], and Lina A. Shehadeh[2,3,6]*

[1]Department of Molecular and Cellular Pharmacology, University of Miami Leonard M. Miller School of Medicine, Miami, FL 33136, USA; [2]Interdisciplinary Stem Cell Institute, University of Miami Leonard M. Miller School of Medicine, Miami, FL 33136, USA; [3]Department of Medicine, Division of Cardiology, University of Miami Leonard M. Miller School of Medicine, Miami, FL 33136, USA; [4]Department of Biochemistry, University of Miami, Coral Gables, FL 33136, USA; [5]Department of Surgery, University of Miami Leonard M. Miller School of Medicine, Miami, FL 33136, USA; and [6]Vascular Biology Institute, University of Miami Leonard M. Miller School of Medicine, Miami, FL 33136, USA

Received 11 December 2014; accepted 27 January 2015; online publish-ahead-of-print 12 February 2015

Time for primary review: 38 days

Aims Activation of an osteogenic transcriptional program contributes to the initiation of aortic calcification in atherosclerosis. The role of microRNAs in regulating aortic calcification is understudied. We tested the hypothesis that miR-30e regulates an osteogenic program in bone marrow-derived mesenchymal stem cells (MSCs), aortic smooth muscle cells (SMCs), and ApoE$^{-/-}$ mice.

Methods and results In aortas of wild-type mice, we found that miR-30e is highly expressed in medial SMCs. In aortas of old ApoE$^{-/-}$ mice, we found that miR-30e transcripts are down-regulated in an inverse relation to the osteogenic markers Runx2, Opn, and Igf2. *In vitro*, miR-30e over-expression reduced the proliferation of MSCs and SMCs while increasing adipogenic differentiation of MSCs and smooth muscle differentiation of SMCs. In MSCs and SMCs over-expressing miR-30e, microarrays and qPCR showed repression of an osteogenic gene panel including Igf2. Inhibiting miR-30e in MSCs increased Igf2 transcripts. In SMCs, IGF2 recombinant protein rescued miR-30e-repressed osteogenic differentiation. Luciferase and mutagenesis assays showed binding of miR-30e to a novel and essential site at the 3′UTR of Igf2. In ApoE$^{-/-}$ mice, injections of antimiR-30e oligos increased Igf2 expression in the aortas and livers and significantly enhanced OPN protein expression and calcium deposition in aortic valves.

Conclusion miR-30e represses the osteogenic program in MSCs and SMCs by targeting IGF2 and drives their differentiation into adipogenic or smooth muscle lineage, respectively. Our data suggest that down-regulation of miR-30e in aortas with age and atherosclerosis triggers vascular calcification. The miR-30e pathway plays an important regulatory role in vascular diseases.

Keywords Osteogenesis • Smooth muscle cells • Calcification • MicroRNA-30e • Mesenchymal stem cells

1. Introduction

Vascular calcification involves induction of an osteogenic program in smooth muscle cells (SMCs).[1,2] Although the origin of osteoblastic cells in atherosclerotic lesions is debated, there is substantial evidence that SMCs enter proliferative, migratory, and synthetic states in response to atherogenic stimuli, and this includes increased expression of bone formation markers such as alkaline phosphatase (ALP) and osteopontin (OPN).[1]

SM22α-Cre-dependent lineage tracing suggests that SMCs may be precursors of osteochondrogenic cells within calcified arterial media and atherosclerotic lesions.[3] Therefore, in this study, we analysed both aortic SMCs and bone marrow-derived mesenchymal stem cells (MSCs), because both are possible targets for osteogenic differentiation. While SMCs and MSCs originate from different cellular compartments, both cell types exhibit plasticity and the capability for osteogenic differentiation. To our knowledge, comparing the responses of these two cell types in parallel to osteogenic stimulation has not been studied and any

* Corresponding author. Tel: +1 305 243 0867; fax: +1 305 243 3906, Email: lshehadeh@med.miami.edu

distinguishing responses of either may be important to understand the mechanism, aetiology, and cellular origins of vascular calcification.

Recent reports define 'osteomiRs' as microRNAs with impressive biomarker and/or functional roles in the osteogenic differentiation process of MSCs.[4–6] All members of the miR-30 family (with the possible exception of miR-30e) were shown to inhibit osteoblast differentiation of MSCs by targeting Smad1 and Runx2.[7] Most recently, miR-30e was reported to induce adipogenic differentiation and reduce osteogenic differentiation in stromal cells by targeting Lrp6.[8] Interestingly, miR-30e appears to be selectively repressed in the aortas of middle-aged ApoE$^{-/-}$ mice relative to wild-type mice.[9] The global effects of miR-30e on the genome of SMCs or MSCs are not known. In the present study, we demonstrate the following: (i) expression of miR-30e in medial SMCs, (ii) global targets of miR-30e in both MSCs and SMCs, (iii) down-regulation of miR-30e in aged atherosclerotic aortas, (iv) binding of miR-30e to the 3′ UTR of the mRNA of insulin-like growth factor 2 (IGF2) and consequent regulation of gene and protein expression, (v) IGF2 rescue of miR-30e-repressed osteogenic differentiation in SMCs, (vi) miR-30e-mediated reduction of proliferation and induction of the smooth muscle differentiation of SMCs, and (vii) induction of vascular calcification by antimiR-30e *in vivo*.

Together these findings support a model of miR-30e regulation of an IGF2-dependent osteogenic transcriptional program in MSCs, SMCs, and ApoE$^{-/-}$ mice that develop aortic atheromas.

2. Experimental procedures

Reagents are detailed in the Supplementary material online.

2.1 Young and old wild-type and ApoE$^{-/-}$ mice

All experiments involving animals were approved by the Institutional Animal Care and Use Committee at the University of Miami, conforming to NIH guidelines. ApoE$^{-/-}$ mice were bought from Jackson Labs and bred in-house. Young wild-type mice were bought from Jackson labs, and old wild-type mice were bought from the National Institute of Aging. LacZ-miR-30e mice were bought from Jackson Labs. For sacrificing all mice used in this study, isoflurane inhalation followed by cervical dislocation were used. Whole aortas were carefully dissected and pieces of the livers were excised, immediately immersed in RNALater and snap frozen in liquid nitrogen, or fixed in 10% formalin. Tissues were later homogenized in Cell Disruption Buffer (Mirvana Paris kit) for two consecutive 5 min in a Geno/Grinder 2000 homogenizer (OPS Diagnostics LLC, NJ, USA) and used for RNA and protein work. For plaque histology, sections of thoracic plaque were located microscopically, dissected, embedded in OCT, and immediately frozen at −80°C. Frozen OCT blocks were cut using a cryostat (Leica, Buffalo Grove, IL, USA) at 10 μm thickness.

2.2 Alizarin Red and Van Kossa staining of tissue

Slides with 10 μm frozen sections of thoracic plaque or aortic valves were warmed for 10 min at RT then 10 min at 53°C, fixed in 4% PFA for 30 min, dipped in PBS, stained, dipped twice in water, dried, mounted, and sealed.

2.3 Human aortic tissue

Human aortas from healthy donors or atherosclerotic patients were collected under IRB approval at the University of Miami Miller School of Medicine (which includes conformation to the declaration of Helsinki and informed donor/patient consent). The aortas were frozen in OCT and later sectioned at 10 μm thickness for staining as described above.

2.4 OPN immunostaining of tissue

Slides with 10 μm frozen sections of thoracic plaque or aortic roots were warmed for 10 min at RT then 10 min at 53°C, fixed in 4% PFA for 15 min, permeabilized with 0.2% Triton for 30 min, blocked in 10% donkey serum for 30 min, incubated with OPN antibody (R&D) at a concentration 1:50 overnight at 4°C, incubated with Donkey-anti-Goat Alexa Fluor-488 at a concentration 1:200 for 1 h, and mounted with DAPI Antifade (Invitrogen).

2.5 MSC and SMCs isolation and viral transduction

MSCs were isolated from the femurs and tibias of C57Bl6 3-month-old male mice as previously described,[10] and SMCs were isolated from aortic explants of C57Bl6 1-month-old male mice. Cells were passaged 5 times and then transduced with miR-30e or ctrl-miR lentiviral vectors. Puromycin selection was employed to create stable lines. At least three independent MSC or SMC isolations and generation of stable lines were implemented.

2.6 Primary hepatocyte isolation and transfection

C57BL6 mouse was anaesthetized, and inferior vena cava (IVC) was exposed and cannulated. Liver was perfused through IVC with liver perfusion media at 6 mL/min for 5 min and then liver digestion media for 10 min. Liver was excised, transferred to a 100 mm culture dish, torn and shaken with forceps to free digested cells. Cells were passed through a 70 μm strainer, centrifuged at 50 *g* for 2 min at 4°C, and washed twice with William E media. Cells were then nucleofected (Amaxa, Lonza) with either control/SCR or miR-30e plasmids. Finally, transfected cells were plated on collagen I pre-coated 6-well plates. Four hours post plating, media were changed to serum-free culture media.

2.7 Cell proliferation assays

For proliferation assay, lentiviral-transduced MSCs or SMCs were plated in 60 mm tissue culture dishes at a density of 5×10^4 per plate and counted daily for 6 days on a Coulter Counter (Beckman) or a T10 Cell Counter (Biorad). At least three plates were used per time point for each group.

2.8 Transcribing 2′F miR-30e and miR-125b oligos

Templates for the sense and non-sense strands of premiR-30e and premiR-125b were generated as Ultramer DNA oligos (IDT), annealed at 95°C for 5 min, cooled down to room temperature, and then transcribed to 2′F RNA oligos using Durascribe T7 enzyme kit following manufacturer's protocol. Final product was DNase I digested and purified on Acrylamide/Urea gel before transfection into cells.

2.9 Treatment of MSCs with IGF2 recombinant protein

IGF2 recombinant protein was added to cultured MSCs at a 500 ng/mL final concentration. Cells were harvested 1, 2, 4, 6, 8, and 24 h following treatment, and mature miR-30e transcripts were quantified by qPCR.

2.10 Electron microscopy

Cultures were fixed for 20 min in 4% PFA, rinsed in wash buffer three times, and then postfixed in 2% osmium tetroxide in 0.1 M phosphate buffer for 1 h. After buffer rinses, they were dehydrated through a series of graded ethanols and embedded using EMbed (Electron Microscopy Sciences, Hatfield, PA) overnight in a 64°C oven. Silver/gold sections were cut on a Leica Ultracut E (Leica) and stained in uranyl acetate and lead citrate. Images were captured by a Gatan Erlangshen ES1000W camera (Gatan, Pleasanton, CA, USA) in a Philips CM10 electron microscope (FEI, Hillsboro, OR, USA).

2.11 Osteoblastic differentiation

To induce osteoblastic differentiation, after reaching 80% confluency, BM-MSCs at passages 12–19 were cultured in α-MEM (M8042, Sigma) supplemented with 10% FBS, 1% P/S, 0.1 nmol/L dexamethasone (SigmaD4902), 0.01 mmol/L β-glycerophosphate (Sigma G9422), and 0.05 mmol/L ascorbic acid-2-phosphate (Sigma A8960). This method has been reported to induce differentiation through the IGF2 system.[11] Media were changed twice every week. One millilitre of media was collected at the 7-day and 14-day time points for ELISA. For RNA work, cell lysates were collected in Cell Disruption Buffer (Mirvana Kit).

2.12 Adipogenic differentiation

To induce adipogenic differentiation, after reaching 90% confluency, BM-MSCs at passages 12–19 were cultured in Mesencult MSC Basal Medium with Adipogenic Stimulatory Supplement (Stem Cell Technologies) for 10 days. Media were changed twice only.

2.13 IGF2 and BMP2 rescue experiment

SMCs were isolated from 2-month- or 18-month-old mouse aorta and transduced with ct-miR or miR-30e lentivirus. At passage 10, SMC stables were seeded in a 24-well cell culture plate and stimulated to osteogenic differentiation by supplementing cells with osteogenic induction media. IGF2 or BMP2 recombinant protein was added at 500 or 250 ng/mL to wells of SMC + miR-30e stables twice a week during media change. After 2, 2.5, or 4 weeks of osteogenic induction, cells were fixed in 10% formalin for 30 min, rinsed with distilled water, and stained with 2% Alizarin Red solution for 45 min in the dark. Finally, cells were washed with distilled water and microscopic images were taken. Five images were captured per well, and at least three wells were used per group.

2.14 Luciferase 3′UTR assay

Luciferase vectors containing full-length Igf2 (wt or mutant), full-length OPN, or 500 bp of Runx2 3′ UTRs were transfected into 293T or HEPA1-6 cells stably over-expressing miR-30e or ct-miR using Lipofectamine 2000 (Invitrogen). Forty-eight hours post-transfection, cells were assayed for luciferase activities using the Luc-Pair miR dual luciferase assay kit (Genecoepia) and a microplate reader (SpectraMax M5, Sunnyvale, CA, USA). Binding activities were finally reported as Firefly to Renilla luciferase luminescence in the same cells.

2.15 Enzyme-linked immunosorbent assay

For quantification of secreted OPN and IGF2 proteins from MSC cultures, equal volumes of collected media were used. For quantification of aortic OPN protein from ApoE$^{-/-}$ mice, whole aortic lysates were used and normalized to GAPDH Elisa. For quantification of aortic and hepatic IGF2 protein from ApoE$^{-/-}$ mice, lysates were subjected to Elisa and readings were normalized to measured protein concentrations. In all the ELISAs, each biological sample was assayed in duplicates, and a perfect standard curve was generated for measurements and/or quality control.

2.16 Alizarin Red and Oil Red staining of cells

MSC lentiviral stables were seeded in 24-well cell culture plate and stimulated to osteogenic differentiation or adipogenic differentiation by supplementing induction media accordingly. After 10 days, 2 weeks, 2.5 weeks, or 4 weeks of induction, cells were fixed in 10% formalin for 30 min and rinsed with distilled water. For Alizarin Red staining, 2% Alizarin Red solution was applied to each well and left for 45 min in the dark. Finally, cells were washed with water, and microscopic images were obtained. For Oil Red Staining, cells were incubated with 60% isopropanol for 5 min, stained with Oil Red solution for 5 min. Finally, cells were washed with water, and microscopic images were obtained.

2.17 Animal injections and tissue collection

In the first experiment, 5-month-old ApoE$^{-/-}$ male mice fed normal chow received tail vein injections of 0.6 nmol 2′Ome antimiR-30e ($n = 8$) or a scrambled (SCR) control oligo ($n = 7$) every other day for 1 month. A total of 16 injections per mouse were administered. Whole aortas were carefully dissected, and pieces of the livers were excised, immediately immersed in RNALater, and snap frozen in liquid nitrogen. Tissues were later homogenized in Cell Disruption Buffer (Mirvana Paris kit) for two consecutive 5 min in a Geno/Grinder 2000 homogenizer (OPS Diagnostics LLC) and used for RNA and protein work.

In the second experiment, 6-month-old ApoE$^{-/-}$ male and female mice fed on high-fat (HF) chow received tail vein injections of 3 nmol (100 nmol/kg) 2′Ome antimiR-30e ($n = 7$) or PBS ($n = 6$) every other day for 2 months. A total of 36 injections per mouse were administered. For aortic valve collection for histology, hearts were perfused with potassium chloride to arrest in diastole for aortic valve closure, fixed overnight in 4% PFA at 4°C, incubated in 10% sucrose for 4 h at 4°C, incubated in 20% sucrose overnight at 4°C, incubated in 20% sucrose: OCT (50:50) for 3 h at RT, embedded in OCT, and frozen at −80°C. Frozen OCT blocks were cut using a cryostat (Leica) at 10 μm thickness. Livers were collected and processed for RNA and protein work as described above. Liver tissues were also saved in formalin, and 4 μm paraffin sections were stained with H&E and Masson Trichrome staining. Blood was collected, and plasma CRP protein levels were measured using a CRP sandwich Elisa kit (R&D).

In the third experiment, 8-month-old ApoE$^{-/-}$ male and female mice fed on normal chow received tail vein injections of 6 nmol (200 nmol/kg) 2′Ome antimiR-30e ($n = 4$) or PBS ($n = 5$) every day for three consecutive days. Aortic arches were collected and processed for RNA work as described above.

2.18 Animal work

All experiments involving animals were approved by the Institutional Animal Care and Use Committee at the University of Miami. ApoE$^{-/-}$ mice on C57Bl6 background were bought from Jackson Labs and bred in-house. Young C57Bl6 wild-type mice were bought from Jackson labs, and old wild-type mice were bought from the National Institute of Aging.

2.19 Statistics

For all experiments, n refers to the number of individual mice or individual culture plates. All data are expressed as mean ± SEM. P-values were calculated using Student's t-tests. For data in Supplementary material

online, *Figure S1*, we employed ANOVA with Tukey *Post hoc* correction using SPSS 22 software, to compare gene and microRNA expression among the four groups. Repeated symbols represent *P*-values of different orders of magnitude, i.e. $*P < 0.05$, $**P < 0.01$.

3. Results

3.1 miR-30e is expressed in medial SMCs in mouse aorta

To identify the cells that express miR-30e in mouse aortas *in situ*, we performed B-gal staining in aortas of 2-month-old miR-30e-lacZ mice.[12] By co-staining for B-gal, smooth muscle marker (SM1), and endothelial marker (CD34), we found that miR-30e is unequivocally expressed in medial SMCs (*Figure 1*).

3.2 Nuclear transcription factor gamma and hosted miR-30e transcripts are down-regulated with age and atherosclerosis

miR-30e (and miR-30c) sits in intron 5 of nuclear transcription factor gamma (*NFYC*) gene. Mature sequence of miR-30e is conserved across human, mouse, and rat species (see Supplementary material online, *Figure S1A*). To study the dynamics of Nfyc and hosted miR-30e expression with age and atherosclerosis, we collected the full aortas from 'young' 6-month-old ApoE$^{-/-}$ ($n = 7–9$) and WT ($n = 4$) mice, and 'old' 13.5-month-old ApoE$^{-/-}$ ($n = 9–15$) and WT ($n = 3–6$) mice—all on normal chow. We found by qPCR that relative to young wild type, Nfyc and mature miR-30e transcripts are down-regulated in old wild-type and mostly old ApoE$^{-/-}$ aortas (see Supplementary material online, *Figure S1B* and *Table S1*). We also found that the pattern of Nfyc/miR-30e expression is inversely proportional to the expression of the osteogenic genes Runx2, OPN, and IGF2 (see Supplementary material online, *Figure S1B* and *Table S1*). Our finding supports a previous report that miR-30e was the most down-regulated microRNA in the aortas of 10-month-old ApoE$^{-/-}$ vs. wild-type mice.[9] Measuring aortic OPN protein and normalizing to GAPDH, both by sandwich ELISA, we found that OPN protein was significantly up-regulated in ApoE$^{-/-}$ aortas in both young and old mice ($n = 3–15$ per group; see Supplementary material online, *Figure S1C*). Our results confirm previous reports on over-expression of OPN in atherosclerotic arteries.[13–15] In addition, the increase in OPN expression at an early stage of atherosclerosis confirms previous reports on induction of osteogenesis programs during arterial calcification.[16]

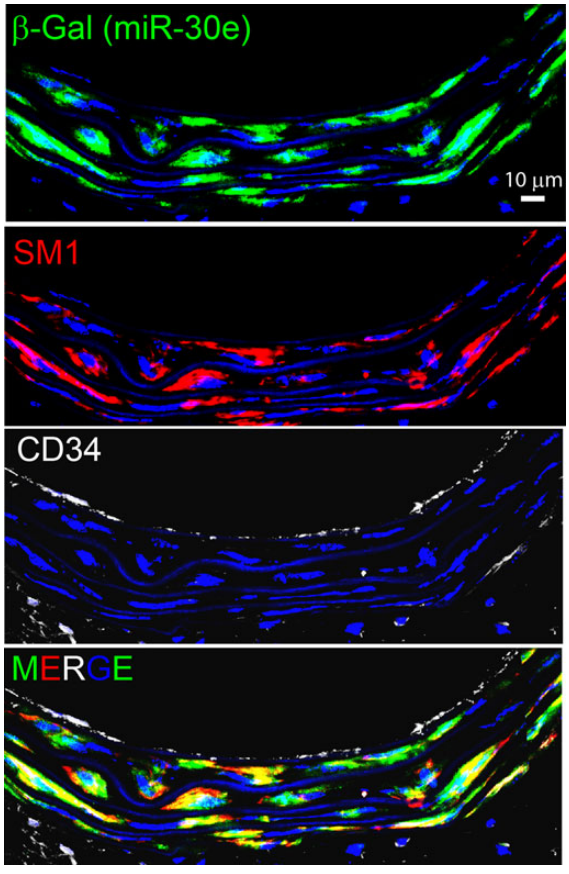

Figure 1 miR-30e is expressed in medial SMCs in mouse aorta. Confocal microscopy shows β-gal staining (corresponding to miR-30e expression) in medial SMCs in 2-month-old mouse thoracic aorta. SM1 and CD34 staining show smooth muscle and endothelial cells, respectively. DAPI/nuclear staining is shown in blue.

3.3 Calcification is evident in plaque of old atherogenic mouse aortas and in medial SMCs of human atherogenic aortas

In young ApoE$^{-/-}$ mice, no calcification is observed in aortic plaque (data not shown). However, in old (13.5 months) ApoE$^{-/-}$ mice, calcium mineralization is clear when aortic plaque is stained with Alizarin Red, Van Kossa, or OPN (*Figure 2A–C*). In human atherosclerotic plaque, on the other hand, arterial (medial) calcification is much stronger than in mouse (*Figure 2D* and *E*). We performed *in situ* hybridization on human normal aortas and confirmed expression of miR-30e in human medial SMCs (*Figure 2F*) as in mouse medial SMCs (*Figure 1*).

3.4 miR-30e drives MSCs towards adipogenic differentiation, and SMCs towards smooth muscle differentiation

We tested proliferation and differentiation potential in MSCs and SMCs stably over-expressing miR-30e vs. ct-miR in normal media. First we recorded cell numbers in 6 consecutive days and found MSCs over-expressing miR-30e exhibited a significant lower proliferation rate at Days 2, 4, and 5 (*Figure 3A*). A slow proliferation rate suggested a tendency towards a differentiation lineage. Our microarray data confirmed adipogenic tendency, by significant over-expression of the two major adipogenic markers fatty acid-binding protein 4 (Fabp4) and peroxisome proliferator-activated receptor gamma (Pparγ) by miR-30e (*Figure 3B*). These results are in line with a very recent report on miR-30e inducing adipogenic differentiation in bone marrow stromal cells.[7,8] Our microarray data showed that in SMCs and MSCs, miR-30e did not cause a significant change in the gene expression of Bmi1 which was reported as regulated by miR-30e*.[17] Similarly, in MSCs, antimiR-30e (equivalent to miR-30e*) did not cause a significant change in the expression of Bmi gene. Therefore, our microarray data suggest that the targeting of Bmi1 by miR-30e could be cell specific and un-related to the miR-30e effects in SMCs and MSCs. In SMCs also, miR-30e delayed proliferation rate at Days 2–6 (*Figure 3C*) and induced smooth muscle differentiation as quantified by western blots of the smooth

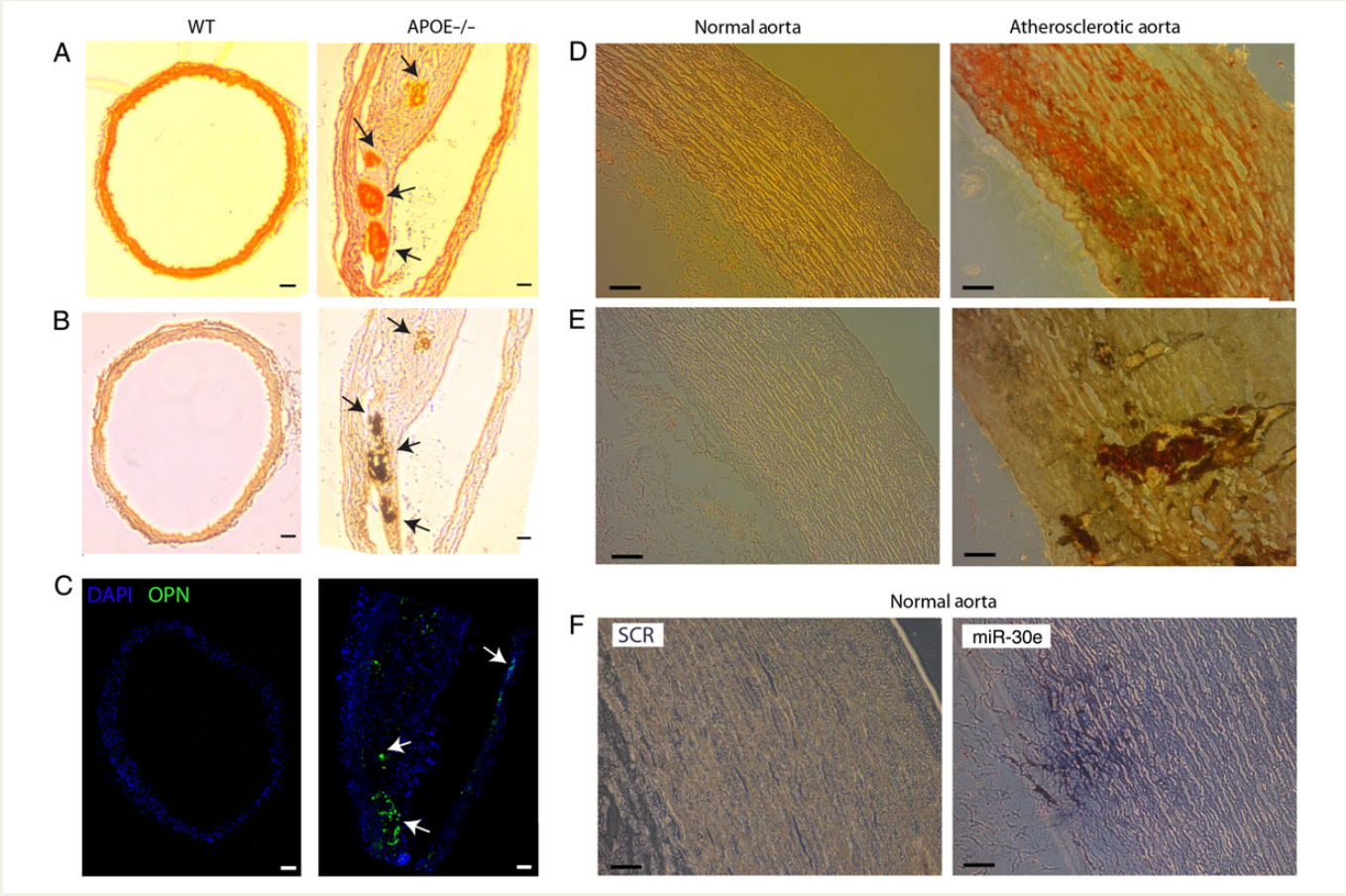

Figure 2 Plaque calcification is evident in old ApoE$^{-/-}$ mice. Plaque calcification is evident in old (13.5 months) ApoE$^{-/-}$ mice on normal diet as visualized by Alizarin Red staining (*A*), Van Kossa staining (*B*), and OPN immunostaining (*C*) of consecutive sections of mouse thoracic aortas. Shown are Alizarin (*D*) and Von Kossa (*E*) staining of normal and atherosclerotic human aortas. miR-30e is expressed in the arterial wall of normal human artery, as shown by *in situ* hybridization (*F*). Scale bar = 100 μm. WT, wild type.

muscle lineage markers smooth muscle 22-alpha (SM22α), calponin 1 (Cnn1), and vinculin (VCL) (*Figure 3D*). Confirming the smooth muscle differentiated, less proliferative phenotype, EM showed reduction by miR-30e of cellular organelles (*Figure 3E*). miR-30e caused significant reduction of mitochondrial count (*Figure 3F*). Our results on miR-30e inducing smooth muscle or adipogenic differentiation while reducing osteogenic differentiation are in line with the concept of a sensitive balance/seesaw that forces the cells to choose one lineage over the other.

3.5 miR-30e reduces osteogenic and increases adipogenic differentiation of MSCs

A major characteristic of osteoblasts is secretion of extracellular matrix protein and formation of calcium–mineral nodules,[18] which is also clinically implicated in atherogenic plaques.[19] We tested calcification in lentiviral-transduced MSCs after 2 weeks of osteogenic induction in osteogenic media. Using Alizarin Red staining, we observed much less calcium deposition in miR-30e over-expressing MSCs (see Supplementary material online, *Figure S2A*). During late osteoblastic differentiation, MSC morphology changed from a spread cell to a narrow calcified cell. Interestingly, EM showed dramatic morphological preservation in MSCs over-expressing miR-30e after 2 weeks of osteogenic differentiation (see Supplementary material online, *Figure S2B*). Thus, miR-30e tremendously reduced osteogenic differentiation of MSCs.

After 10 days of adipogenic differentiation, Oil Red staining showed bigger fat droplets in miR-30e over-expressing MSCs (see Supplementary material online, *Figure S2C*), confirming that miR-30e drives MSCs towards adipogenic differentiation. EM shows huge fat droplets in both MSC groups (see Supplementary material online, *Figure S2D*). In addition, our microarray data confirmed miR-30e down-regulation of Lrp6 (−2.7-fold, $P = 0.02$) which was reported as a mechanism for inducing adipogenic differentiation in stromal cells.[8]

3.6 miR-30e down-regulates an osteogenic gene panel in MSCs

To test the prediction that miR-30e controls MSC differentiation potential, we performed microarrays on MSCs stably over-expressing either a control miR (MSCs + ct-miR) or miR-30e (MSCs + miR-30e). Interestingly, the genes most down-regulated by miR-30e included the bone formation/ossification genes dermatopontin (Dpt), insulin growth factor 2 (Igf2), bone morphogenetic protein 4 (Bmp4), chordin-like 1 (Chrdl1), and immunoglobulin superfamily, member 10 (Itgsf10)—listed in Supplementary material online, *Table S2*. To establish the detailed dynamics of

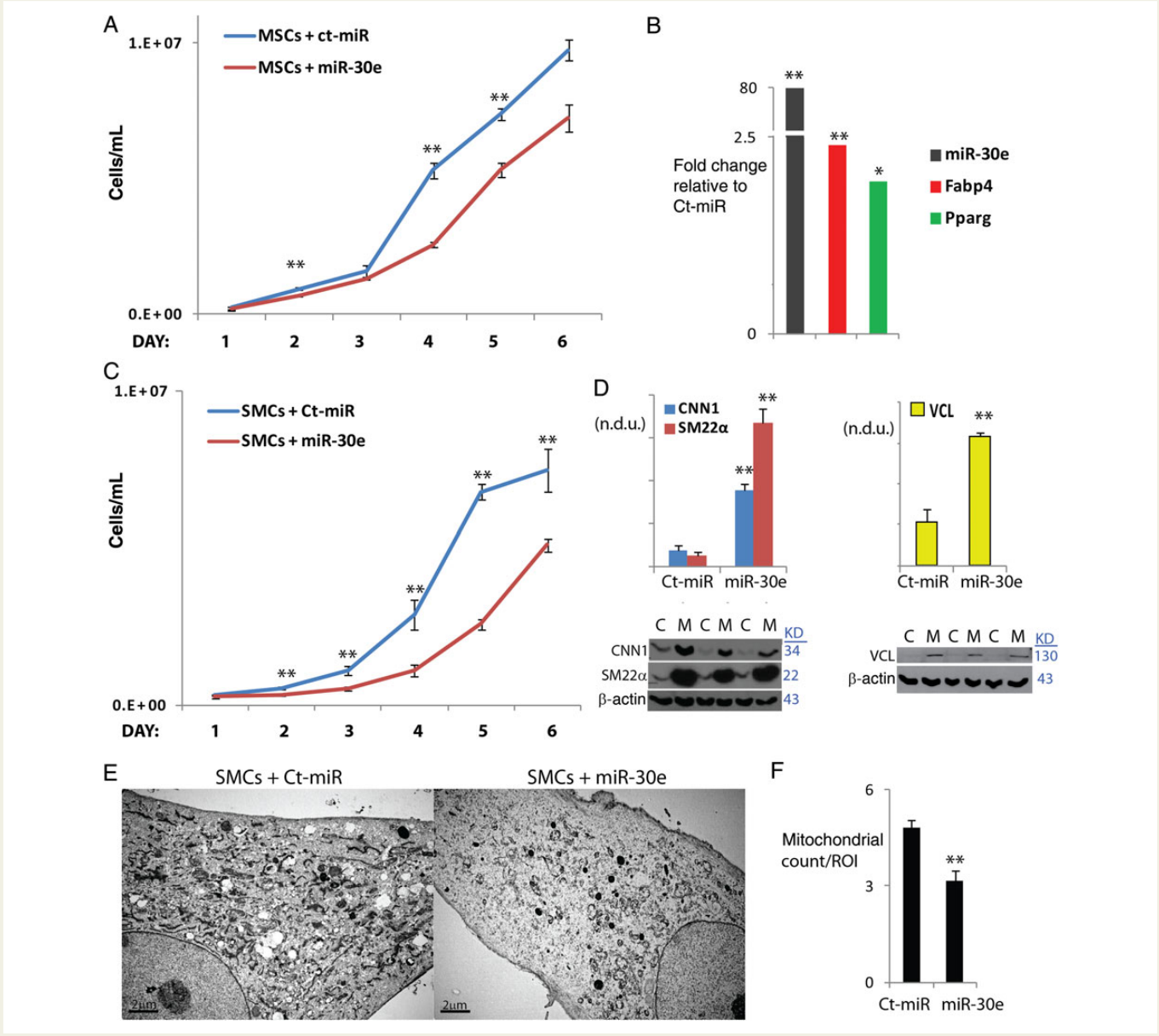

Figure 3 miR-30e over-expression reduces proliferation of MSCs and SMCs and drives adipogenic and smooth muscle differentiation, respectively. (*A*) MSCs stably over-expressing miR-30e show a significant delay in cell proliferation. (*B*) The two main adipogenic markers, Fabp4 and Pparg, are significantly induced in MSCs stably over-expressing miR-30e, as shown by the bar graph from microarray analysis. (*C*) SMCs stably over-expressing miR-30e show a significant delay in cell proliferation. (*D*) Smooth muscle markers, CNN1, SM22α, and VCL, are significantly induced in SMCs stably over-expressing miR-30e, as shown by the western blot and corresponding densitometry. (*E*) EM shows reduction of organelles in SMCs over-expressing miR-30e especially in mitochondria (*F*). $n = 3$ per group; experiments repeated at least twice. Data are mean ± SEM. $^{*}P < 0.05$; $^{**}P < 0.01$.

osteogenic induction in MSCs, we initially used osteogenic media that is 1000-fold less intense (in dexamethasone and β-glycerophosphate concentration) than standard osteogenic recipe. We believe that this 'light' osteogenic media is more physiologically relevant and would allow to better capture the dynamics of osteogenesis. As early as 1 day after osteogenic induction and peaking at 2 weeks, MSCs over-expressed a panel of eight osteogenic markers including Igf2 (see Supplementary material online, *Figure S3A*). Note that Bmp4 (1.6-fold; $P = 0.0034$) and Alp (1.6-fold; $P = 0.05$) transcripts were significantly increased at Day 1. Starting at Day 2, most of the eight genes were up-regulated, especially Igf2 which was mostly induced at Day 5 (50.1-fold; $P = 0.0003$) and Day 14 (115.6-fold; $P = 0.0008$; see Supplementary material online, *Figure S3A*). This supports a very recent report on Igf2 being the most induced gene in mouse aortic SMCs after osteogenic differentiation.[20]

Most interestingly, this osteogenic panel (eight genes) was tightly regulated by miR-30e. We quantified by qPCR the gene expression of the osteogenic panel in MSCs transiently transfected with 0.1, 1, or 10 nmol/L of 2F' miR-30e oligos. Results confirmed the reduction of the osteogenic panel (including ALP) by miR-30e in a dose-dependent manner (see Supplementary material online, *Figure S3B* and *Table S3*).

Next we tested these same genes in MSCs stably over-expressing miR-30e before and after osteogenic differentiation. We found that

Dpt (−11.3-fold, $P = 0.03$), Dcn (−12.9-fold, $P = 0.01$), Bmp4 (−5.2-fold, $P = 0.01$), and Igf2 (−21.7-fold, $P = 0.02$) transcript levels were significantly lower in MSCs over-expressing miR-30e relative to the control treated cells (see Supplementary material online, *Figure S3C*—left panel). After 2-week osteogenic differentiation, gene expressions of these osteogenic markers (as well as OPN, Runx2, and Bmp4) went significantly up in the control group as expected but were only modestly increased in the miR-30e-transduced cells (see Supplementary material online, *Figure S3C*—right panel). Igf2 transcripts were significantly down-regulated in MSCs over-expressing miR-30e relative to the controls in the differentiated cells (−37.7-fold; $P = 0.04$), suggesting a leading role for IGF2 in the osteogenic panel.

3.7 Igf2 is regulated by miR-30e and antimiR-30e in mirror directions

To study the effect of over-expressing and knocking down miR-30e on MSCs in an unbiased manner, we performed global gene expression microarray studies using four groups, MSCs stably transduced with ct-miR or miR-30e lentivirus and MSCs transiently transfected with LNA scrambled or antimiR-30e oligos (GEO GSE65435). To identify miR-30e targets that showed reversible regulation with the antimiR-30e, we implemented Venn analysis and identified Igf2 as one of the seven targets that are repressed by miR-30e and induced by antimiR-30e, respectively (see Supplementary material online, *Figure S4A* and *B*). To find common genes regulated by miR-30e in MSCs and SMCs,

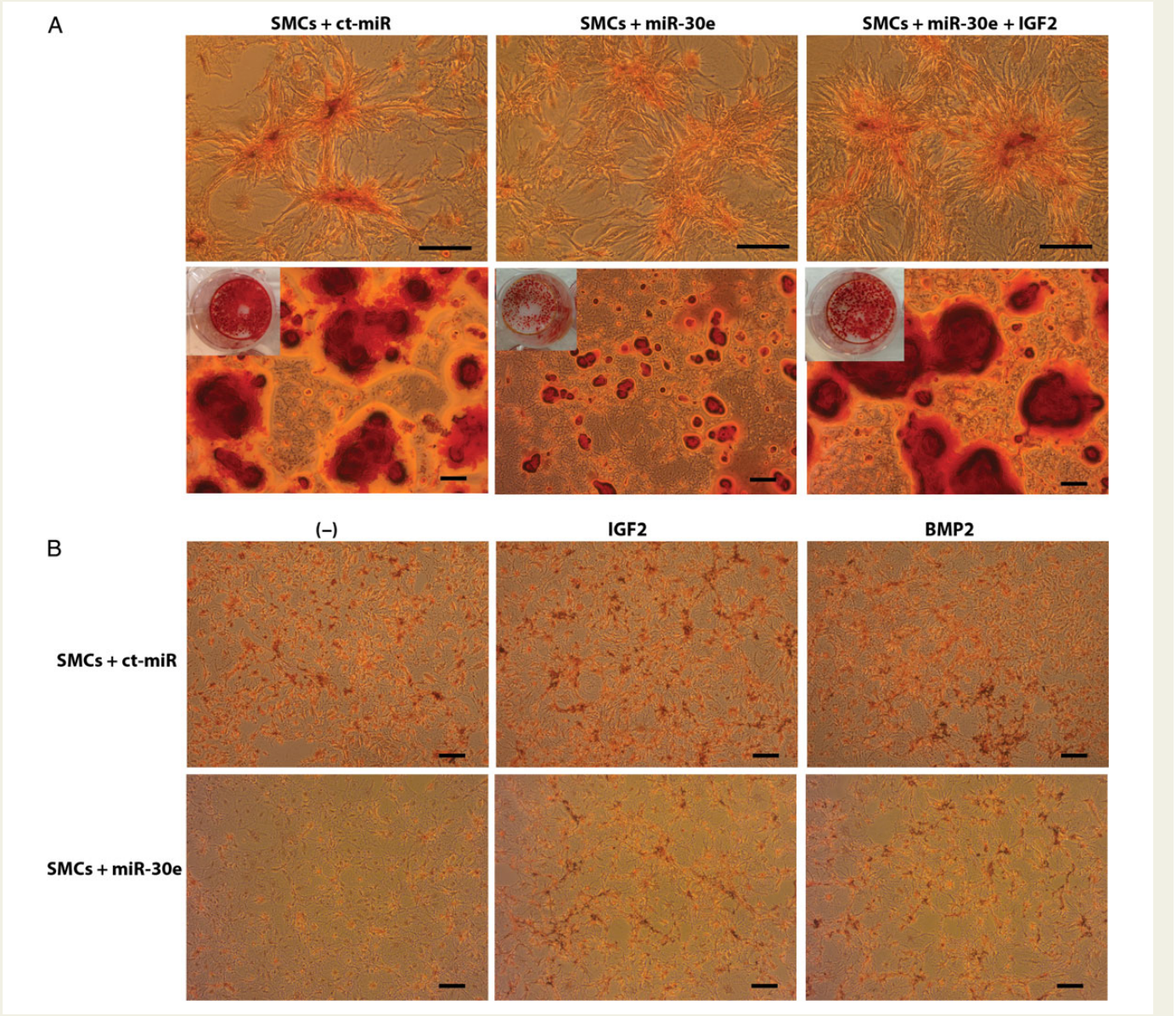

Figure 4 IGF2 recombinant protein rescues miR-30e-repressed osteogenesis in SMCs. (*A*) SMCs stably over-expressing miR-30e show repression of osteogenic differentiation as measured by Alizarin Red 2 weeks (top row) and 4 weeks (second row) after osteogenic induction. Addition of IGF2 recombinant protein at 500 mg/mL rescues osteogenic differentiation in the SMCs over-expressing miR-30e. (*B*) At 2.5 weeks of osteogenic differentiation, IGF2 as well as BMP2 recombinant protein (both at 250 ng/mL) rescue osteogenic differentiation in the SMCs over-expressing miR-30e. Images are representative of at least three experiments per group. Scale bar = 100 μm.

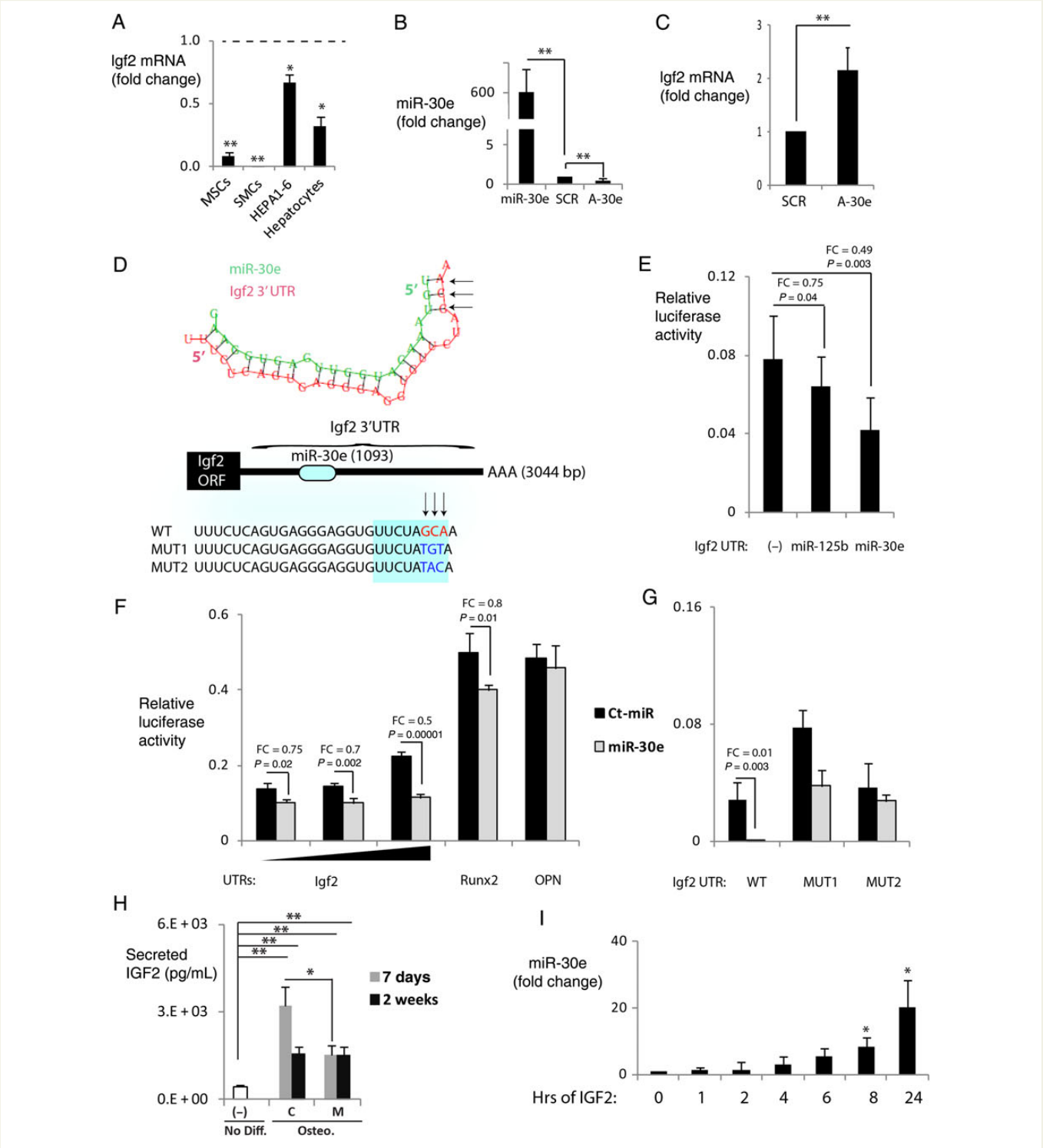

Figure 5 miR-30e directly targets and regulates Igf2 transcripts and proteins *in vitro* and *in vivo*. (*A*) miR-30e over-expression reduces Igf2 transcripts in MSC, SMCs, Hepa1-6 cells, and mouse primary hepatocytes—all relative to their ct-miR groups—as shown by qPCR. (*B*) qPCR shows successful over-expression and knock down of miR-30e in MSCs using 2′F miR-30e or LNA antimiR-30e oligo 2-day transfections, respectively. (*C*) Transfection with antimiR-30e oligos for 2 days in MSCs causes up-regulation of Igf2 transcripts as shown by qPCR. (*D*) Shown is the secondary structure of the binding of miR-30e mature sequence to Igf2 3′UTR as predicted by RNAHybrid software. Arrows point to mutation sites at Igf2 3′UTR used to generate two mutant sequences. (*E*) Using 2′F miR-30e or miR-125 (positive control) oligos in Hepa1-6 cells, luciferase assay shows binding of miR-30e to the Igf2 3′UTR. (*F* and *G*) Using miR-30e or ct-miR lentiviral Hepa1-6 or 293T stables (*G*), luciferase assay shows binding of miR-30e to 3′UTR of Igf2 and Runx2 (positive control), but not OPN nor mutant Igf2 constructs. $n = 4–5$ per group. (*H*) Secreted Igf2 protein levels are significantly reduced in miR-30e-transduced MSCs after 7 days of osteogenic differentiation, as measured by sandwich ELISA. $n = 4$ per group. (*I*) Treatment of MSCs with IGF2 recombinant protein (500 ng/mL) induces miR-30e transcripts as measured by qPCR. $n = 4$ per group. For all experiments, data are mean ± SEM; $^{*}P < 0.05$, $^{**}P < 0.01$. SCR, scrambled oligo; A-30e, AntimiR-30e; MUT, mutant.

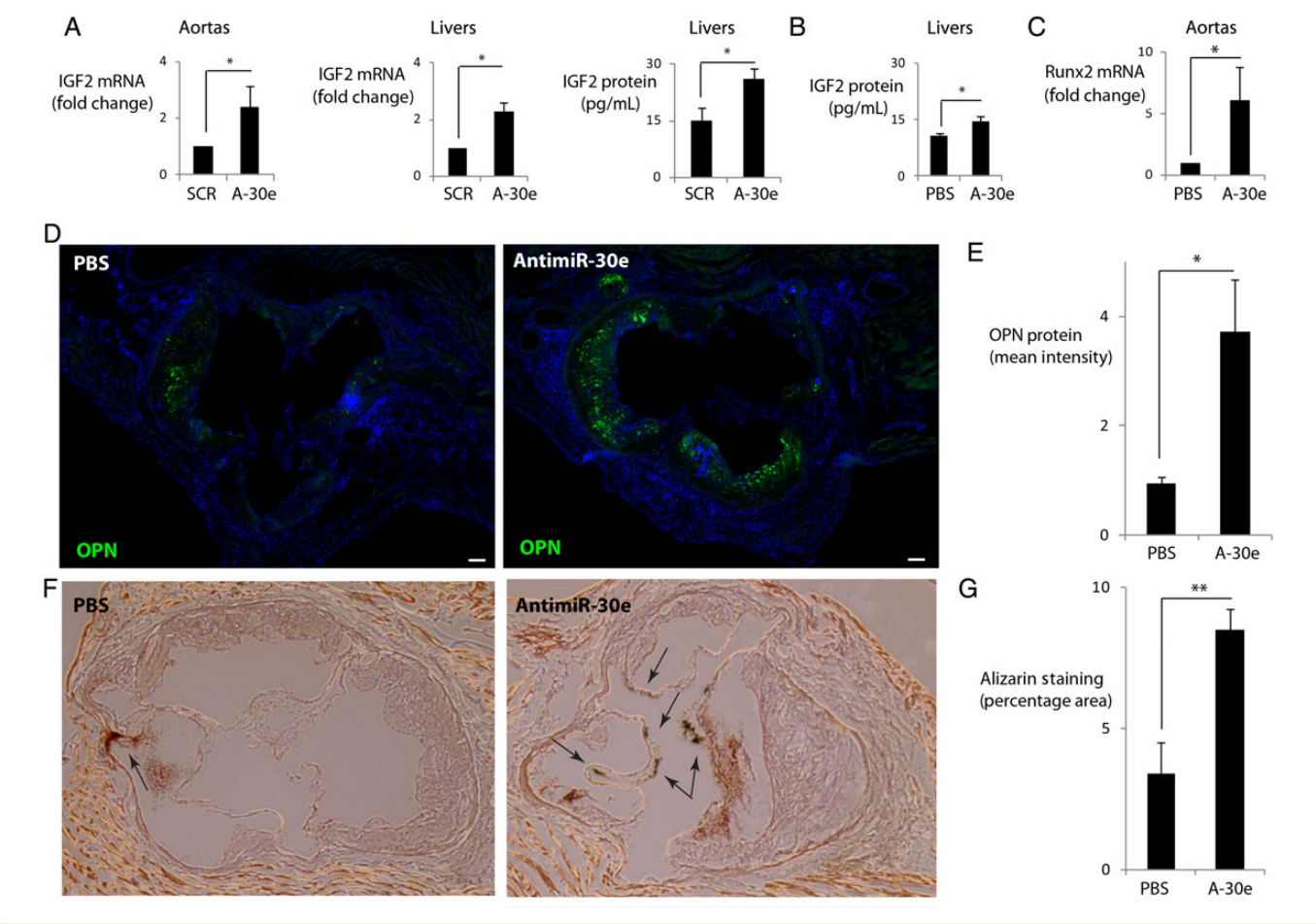

Figure 6 AntimiR-30e injections in ApoE$^{-/-}$ mice triggers calcification in aortic valves. (*A*) Systematic administration of 0.6 nmol antimiR-30e oligos in 6-month-old ApoE$^{-/-}$ mice on normal chow causes significant up-regulation of Igf2 aortic and hepatic mRNA and Igf2 hepatic protein as measured by qPCR and sandwich ELISA, respectively ($n = 4–7$ mice per group). (*B*) Systematic administration of 3 nmol antimiR-30e oligos in 8-month-old ApoE$^{-/-}$ mice on HF diet causes significant up-regulation of hepatic IGF2 hepatic protein as measured by sandwich ELISA ($n = 6–7$ mice per group). (*C*) Systemic administration of 6nmols of antimiR-30e oligos in 8 mo ApoE$^{-/-}$ mice on normal chow causes significant up-regulation of aortic Runx2 mRNA after 3 days as measured by qPCR ($n = 4–5$ per group). Systematic administration of 3 nmol antimiR-30e oligos in 8-month-old ApoE$^{-/-}$ mice on HF diet causes significant induction of OPN protein expression in aortic valves as seen by OPN immunostaining (*D*) and corresponding quantification (*E*) and Alizarin Red staining (*F*) and corresponding quantification (*G*). Images are representative of $n = 5$ mice per group. Scale bar = 100 μm. A-30e, AntimiR-30e. Data are mean ± SEM; *$P < 0.05$.

we also implemented microarrays (GEO GSE65435) and Venn analysis and found that Igf2 and related genes were down-regulated in both MSCs and SMCs relative to their controls (see Supplementary material online, *Figure S4C*). Using GO analysis on the genes differentially repressed by miR-30e in MSCs, we found that 'Kinase Related Activity', 'Lectin-Like Receptor', 'Insulin-Like Growth Factor Receptor', and 'Protein Binding' were the four most represented molecular functions regulated by miR-30e ($P < 0.05$, see Supplementary material online, *Figure S5*). The microarray data further supported the role of miR-30e in regulating an osteogenic program in MSCs and specifically involving Igf2.

qPCR validated the microarray results on Igf2; miR-30e over-expression repressed Igf2 transcripts in MSCs, SMCs, Hepa1-6 mouse hepatocarcinoma cells, and primary hepatocytes (*Figure 5A*). AntimiR-30e, which reduced miR-30e levels (−6.0-fold, $P = 0.01$; *Figure 5B*), up-regulated Igf2 transcripts relative to control SCR (2.3-fold, $P = 0.04$; *Figure 5C*) and miR-30e oligo groups.

3.8 IGF2 recombinant protein rescues miR-30e-repressed osteogenesis in SMCs

To validate that IGF2 is indeed a mechanism by which miR-30e reduces osteogenesis in SMCs, we generated SMCs stably over-expressing miR-30e or a ct-miR and cultured them in osteogenic media for several weeks. SMCs stably over-expressing miR-30e show repression of osteogenic differentiation as measured by Alizarin Red 2 and 4 weeks after osteogenic induction. Addition of IGF2 recombinant protein (500 mg/mL) rescued osteogenic differentiation in the SMCs over-expressing miR-30e (*Figure 4A*). To test the ability of another potent osteogenic agent to rescue miR-30e-repressed osteogenesis, we performed a 2.5-week osteogenic experiment in SMC stables and treated with IGF2 or BMP2 (both at 250 mg/mL). Interestingly, like IGF2, BMP2 also restored osteogenesis in SMCs over-expressing miR-30e. While our microarray data did not show that miR-30e regulates Bmp2 gene expression, the results from this rescue experiment

suggest that IGF2 and BMP2 share common downstream osteogenic effectors that were blocked by miR-30e. This is not surprising since both IGF2 and Bmp2, for example, up-regulate Runx2[21,22] which is also a primary target of miR-30e (*Figure 5F*).[8]

3.9 miR-30e binds to and represses Igf2 transcripts and protein *in vitro* and *in vivo*

To determine whether Igf2 mRNA is the direct target of miR-30e, we first confirmed using RNAHybrid software that miR-30e has a predicted binding site at the murine Igf2 3′UTR (*Figure 5D*). Then, we launched a series of Firefly/Renilla luciferase binding assay experiments in multiple systems using the wild-type and two mutant Igf2 3′ UTR constructs (*Figure 5D*). In HEPA1-6 cells, transfection with 2′F miR-30e oligos caused significant reduction in normalized luciferase activity (0.49-fold, $P = 0.0003$) relative to the control blank group, even more reduction than that caused by the positive control miR-125b[23] (0.75-fold, $P = 0.04$; *Figure 5E*). In HEPA1-6 cell stably over-expressing miR-30e or a control miR, luciferase activity was reduced in the miR group relative to the ct-miR group in a dose-dependent manner with increasing concentrations of the wild-type 3′UTR Igf2 construct, and also with the positive control construct Runx2 that has a predicted site for miR-30e, but not with the OPN construct (*Figure 5F*). Interestingly, luciferase activity showed stronger binding of miR-30e to the Igf2 3′UTR construct than Runx2 which has been reported to being regulated by the other miR-30 family members.[7,24] In addition, our results show no binding of miR-30e to the 3′UTR of OPN which further suggests that the repression of OPN by miR-30e is indirect and possibly downstream of Igf2 regulation by miR-30e.

Previous investigations on microRNA binding principles revealed the importance and sufficiency of complementarity between 5′ end of miRNA mature sequence and its target gene, specifically from the first to the eighth base pair in the complementary sequence,[25] recognized as seed sequence. Therefore, we generated two mutant constructs of the Ig2 3′UTR at the nucleotides (nts) corresponding to the first three bases of the binding miR-30e seed sequence located 1093–1095 nt of Igf2 3′UTR (*Figure 5D*). In 293T cells stably over-expressing miR-30e or a ct-miR lentivirus, luciferase activity was significantly reduced by the wt Igf2 3′ UTR construct but not by the two mutant constructs (*Figure 5G*). These results collectively confirm that miR-30e binds directly to Igf2 3′UTR and represses Igf2 gene expression.

Next we quantified IGF2 protein expression with over-expression of miR-30e. Secreted IGF2 protein levels were significantly and dramatically increased at 7-day osteogenic differentiation in control MSCs (637.4-fold relative to un-differentiated group; $P = 0.001$), but nearly completely repressed in miR-30e-transduced MSCs (0.5-fold relative to ct-miR differentiated group; $P = 0.02$; *Figure 5H*).

3.10 IGF2 induces miR-30e expression in MSCs

Interestingly, we found that treatment of MSCs with IGF2 recombinant protein (500 ng/mL) quickly induced the expression of miR-30e ($n = 4$ per group, $P = 0.02$; *Figure 5I*). This suggests that miR-30e and IGF2 function in a feedback loop and could explain the non-perfect correlation between miR-30e and its host gene Nfyc transcripts (see Supplementary material online, *Figure S1B*).

3.11 AntimiR-30e induces IGF2 expression and significant calcification in ApoE$^{-/-}$ mice

To study the effect of miR-30e on Igf2 and associated calcification *in vivo*, we injected 5-month-old ApoE$^{-/-}$ mice with 0.6 nmol/injection 2′O-Me antimiR-30e oligos ($n = 8$) or SCR oligos ($n = 7$). We found that antimiR-30e caused significant up-regulation of Igf2 transcripts in aortas (FC = 2.4; $P = 0.03$) and livers (FC = 2.3; $P = 0.03$), and Igf2 protein in livers (FC = 1.7; $P = 0.04$) relative to the Scr group (*Figure 6A*).

Even with the up-regulated aortic Igf2 transcripts in the treated mice, we could not detect IGF2 protein in the aortas. This could be due to the young age of the mice, the quick extracellular secretion of IGF2, and/or the expression of IGF2 protein mainly in the livers.

Injection of 6-month-old ApoE$^{-/-}$ mice with a higher dosage of antimiR-30e (3 nmol or 100 nmol/kg or 0.6 mg/kg per injection, $n = 7$) continued to induce IGF2 protein expression in the livers (*Figure 6B*) and also induced significant calcification in the aortic valves relative to the PBS-injected group as measured by OPN immunostaining (FC = 3.9, $P = 0.02$, $n = 5$ mice per group; *Figure 6D* and *E*) and Alizarin staining (FC = 2.5, $P = 0.004$, $n = 5–6$ per group; *Figure 6F* and *G*). It is quite remarkable that such a low dosage (0.6 mg/kg) of antimiR-30e oligos (in comparison to published dosages used *in vivo* that range between 2.5 and 80 mg/kg) can trigger valvular calcification. To investigate any side effects of 100 nmol/kg antimiR-30e injections, we performed liver pathology using H&E (see Supplementary material online, *Figure S6A*) and Masson Trichrome (see Supplementary material online, *Figure S6B*) staining. We also measured levels of plasma CRP, a marker of inflammation (see Supplementary material online, *Figure S6C*), and body weights (see Supplementary material online, *Figure S6D*). None were affected by the 100 nmol/kg (3 nmol) dosage of antimiR-30e injections ($n = 7$) relative to PBS injections ($n = 6$). In addition, no behavioural changes were observed during treatments, and no gross changes in organs were observed during necropsy.

To check for immediate changes in Runx2 expression by antimiR-30e, we injected 8-month-old ApoE$^{-/-}$ mice on normal chow with 6 nmol antimiR-30e oligos ($n = 4$) or PBS ($n = 5$) once daily for three consecutive days and collected aortic arches. AntimiR-30e caused significant up-regulation of aortic Runx2 mRNA after 3 days as measured by qPCR (FC = 6.1; $P = 0.02$; *Figure 6C*).

4. Discussion

We report that miR-30e is highly expressed in medial SMCs in adult mouse normal aortas (*Figure 1*). We found that Nfyc and hosted miR-30e transcripts are down-regulated in aged mouse atherosclerotic aortas. Interestingly, Nfyc expression was also reported to be down-regulated in the blood of patients with coronary artery disease (CAD) and predicted the extent of CAD.[26] Our results are consistent with previous reports that miR-30e is down-regulated in aortas of middle-aged ApoE$^{-/-}$ mice,[9] human thoracic dissections,[27] and brains of calorie-restricted aging mice.[28] We report for the first time that age and atherosclerosis simultaneously regulate miR-30e. Global gene expression in SMCs and MSCs that over- or under-express miR-30e indicate that miR-30e regulates a unique osteogenic panel of at least eight genes in MSCs, with Igf2 being the shared target across several cell types (MSCs, SMCs, hepatocellular carcinoma cells, and primary hepatocytes). Our results on the anti-osteogenic effects of miR-30e are consistent with recent literature.[7,8]

A novel finding is that miR-30e is pro-smooth muscle differentiated phenotype, lack of which leads to pathogenesis of vasculo-proliferative disease such as atherosclerosis and resteonosis. In SMCs, miR-30e reduces proliferation and organelle count, and increases smooth muscle lineage markers (*Figure 3*), thereby inducing smooth muscle differentiation.

One of the most interesting findings in our study is the identification of IGF2 as a primary target of miR-30e, and that IGF2 rescued the osteogenic phenotype repressed by miR-30e in SMCs. IGF2 is a protein hormone that has been implicated in atherogenesis. IGF2 knock-out ApoE$^{-/-}$ mice showed a significant attenuation of atherogenic plaque formation and development, while IGF2 transgenic ApoE$^{-/-}$ mice showed increased atherosclerotic lesions.[29] We show that antimiR-30e induces expression of IGF2 in aortas and livers of ApoE$^{-/-}$ mice (*Figure 6A* and *B*), accompanied by calcification of the aortic valves (*Figure 6D–G*). IGF2 is a major aging and osteogenic factor,[21,30–33] making it a clinically desirable target for treating age-related calcification. Moreover, it has been proposed that IGF2 contributes to the development of a variety of seemingly unrelated cancers that appear with advanced age.[34]

We postulate that miR-30e is a major regulator of osteogenic differentiation in MSCs and SMCs by targeting IGF2 through a novel miR-30e binding site in the 3′UTR of IGF2 mRNA. IGF2 also induces the expression of miR-30e in a feedback loop, which could explain the non-perfect correlation of Nfyc and hosted miR-30e transcripts (see Supplementary material online, *Figure S1B*). Complementing its anti-osteogenic role, miR-30e induces adipogenic differentiation of MSCs by inducing Fabp4 and Ppar-γ, and by reducing Lrp6.[8] In SMCs, miR-30e reduces proliferation and increases smooth muscle lineage markers, thereby inducing smooth muscle differentiation. Direct and/or indirect mechanisms by which miR-30e promotes differentiation in MSCs and SMCs are still to be identified. It is possible the repression of Runx2 by miR-30e may be responsible for the miR-30e-activated smooth muscle differentiation in SMCs. This is because Runx2 interacts with SRF to promote dissociation of the SRF-Myocd complex attenuating activation of smooth muscle lineage genes.[32] Limitations of our study include lack of investigation of the effect of miR-30e, IGF2, and Runx2 on the activity of the promoter and 3′UTR regions of the smooth muscle and adipogenic genes that were found profoundly induced by miR-30e. In conclusion, our study provides evidence that IGF2, a calcification-, atherogenic-, cancer-, proliferation-, and aging-related molecule, is a primary, novel and clinically desirable target of miR-30e. Therefore, regulation of the miR-30e pathway could be critical for multiple diseases.

Supplementary material

Supplementary material is available at *Cardiovascular Research* online.

Acknowledgements

We thank Dr Keith Webster for careful review of the manuscript. We also thank the Electron Microscope Core Facility at the University of Miami Miller School of Medicine for their services. We thank Dr Maria Bulina from the Imaging Core Facility for her assistance with quantification of staining.

Conflict of interest: Dr Shehadeh and the University of Miami hold a patent on The Use of miR-30e to Treat Vascular Lesions.

Funding

This work was supported by the following grants to LAS: National Institute of Health (K01 AG040468), State of Florida (3KN05), Florida Heart Research Institute, American Heart Association (Scientist Development Grant 0930169N), and American Federation for Aging Research (M1001096). J.M.H. is supported by NIH grants (R01HL110737-01, R01HL107110, UM1HL113460, R01HL084275) and the Starr Foundation. R.I.V-P. is supported by NIH grants (RO1HL109582 and RO1DK098511). W.D. is supported by an AHA predoctoral fellowship (15PRE22450019).

References

1. Johnson RC, Leopold JA, Loscalzo J. Vascular calcification: pathobiological mechanisms and clinical implications. *Circ Res* 2006;**99**:1044–1059.
2. Cho HJ, Lee HJ, Song MK, Seo JY, Bae YH, Kim JY, Lee HY, Lee W, Koo BK, Oh BH, Park YB, Kim HS. Vascular calcifying progenitor cells possess bidirectional differentiation potentials. *PLoS Biol* 2013;**11**:e1001534.
3. Naik V, Leaf EM, Hu JH, Yang HY, Nguyen NB, Giachelli CM, Speer MY. Sources of cells that contribute to atherosclerotic intimal calcification: an in vivo genetic fate mapping study. *Cardiovasc Res* 2012;**94**:545–554.
4. Eguchi T, Watanabe K, Hara ES, Ono M, Kuboki T, Calderwood SK. Ostemir: a novel panel of microrna biomarkers in osteoblastic and osteocytic differentiation from mesencymal stem cells. *PLoS ONE* 2013;**8**:e58796.
5. Huang J, Zhao L, Xing L, Chen D. Microrna-204 regulates runx2 protein expression and mesenchymal progenitor cell differentiation. *Stem Cells* 2010;**28**:357–364.
6. Eskildsen T, Taipaleenmaki H, Stenvang J, Abdallah BM, Ditzel N, Nossent AY, Bak M, Kauppinen S, Kassem M. Microrna-138 regulates osteogenic differentiation of human stromal (mesenchymal) stem cells in vivo. *Proc Natl Acad Sci USA* 2011;**108**:6139–6144.
7. Wu T, Zhou H, Hong Y, Li J, Jiang X, Huang H. Mir-30 family members negatively regulate osteoblast differentiation. *J Biol Chem* 2012;**287**:7503–7511.
8. Wang J, Guan X, Guo F, Zhou J, Chang A, Sun B, Cai Y, Ma Z, Dai C, Li X, Wang B. Mir-30e reciprocally regulates the differentiation of adipocytes and osteoblasts by directly targeting low-density lipoprotein receptor-related protein 6. *Cell Death Dis* 2013;**4**:e845.
9. Han H, Wang YH, Qu GJ, Sun TT, Li FQ, Jiang W, Luo SS. Differentiated mirna expression and validation of signaling pathways in apoe gene knockout mice by cross-verification microarray platform. *Exp Mol Med* 2013;**45**:e13.
10. Gomes SA, Rangel EB, Premer C, Dulce RA, Cao Y, Florea V, Balkan W, Rodrigues CO, Schally AV, Hare JM. S-nitrosoglutathione reductase (gsnor) enhances vasculogenesis by mesenchymal stem cells. *Proc Natl Acad Sci USA* 2013;**110**:2834–2839.
11. Pierce AL, Dickey JT, Felli L, Swanson P, Dickhoff WW. Metabolic hormones regulate basal and growth hormone-dependent igf2 mrna level in primary cultured coho salmon hepatocytes: effects of insulin, glucagon, dexamethasone, and triiodothyronine. *J Endocrinol* 2010;**204**:331–339.
12. Park CY, Jeker LT, Carver-Moore K, Oh A, Liu HJ, Cameron R, Richards H, Li Z, Adler D, Yoshinaga Y, Martinez M, Nefadov M, Abbas AK, Weiss A, Lanier LL, de Jong PJ, Bluestone JA, Srivastava D, McManus MT. A resource for the conditional ablation of microrna in the mouse. *Cell Rep* 2012;**1**:385–391.
13. O'Brien KD, Kuusisto J, Reichenbach DD, Ferguson M, Giachelli C, Alpers CE, Otto CM. Osteopontin is expressed in human aortic valvular lesions. *Circulation* 1995;**92**:2163–2168.
14. Kwon HM, Hong BK, Kang TS, Kwon K, Kim HK, Jang Y, Choi D, Park HY, Kang SM, Cho SY, Kim HS. Expression of osteopontin in calcified coronary atherosclerotic plaques. *J Korean Med Sci* 2000;**15**:485–493.
15. Majumdar R, Miller DV, Ballman KV, Unnikrishnan G, McKellar SH, Sarkar G, Sreekumar R, Bolander ME, Sundt TM 3rd. Elevated expressions of osteopontin and tenascin c in ascending aortic aneurysms are associated with trileaflet aortic valves as compared with bicuspid aortic valves. *Cardiovasc Pathol* 2007;**16**:144–150.
16. Watson KE, Bostrom K, Ravindranath R, Lam T, Norton B, Demer LL. Tgf-beta 1 and 25-hydroxycholesterol stimulate osteoblast-like vascular cells to calcify. *J Clin Invest* 1994;**93**:2106–2113.
17. Sugihara H, Ishimoto T, Watanabe M, Sawayama H, Iwatsuki M, Baba Y, Komohara Y, Takeya M, Baba H. Identification of mir-30e* regulation of bmi1 expression mediated by tumor-associated macrophages in gastrointestinal cancer. *PLoS ONE* 2013;**8**:e81839.
18. Bilousova G, Jun du H, King KB, De Langhe S, Chick WS, Torchia EC, Chow KS, Klemm DJ, Roop DR, Majka SM. Osteoblasts derived from induced pluripotent stem cells form calcified structures in scaffolds both in vitro and in vivo. *Stem Cells* 2011;**29**:206–216.
19. Rajamannan NM, Subramaniam M, Rickard D, Stock SR, Donovan J, Springett M, Orszulak T, Fullerton DA, Tajik AJ, Bonow RO, Spelsberg T. Human aortic valve calcification is associated with an osteoblast phenotype. *Circulation* 2003;**107**:2181–2184.
20. Zhu D, Mackenzie NC, Millan JL, Farquharson C, Macrae VE. Upregulation of igf2 expression during vascular calcification. *J Mol Endocrinol* 2014;**52**:77–85.

21. Hardouin SN, Guo R, Romeo PH, Nagy A, Aubin JE. Impaired mesenchymal stem cell differentiation and osteoclastogenesis in mice deficient for igf2-p2 transcripts. *Development* 2011;**138**:203–213.
22. Lee KS, Kim HJ, Li QL, Chi XZ, Ueta C, Komori T, Wozney JM, Kim EG, Choi JY, Ryoo HM, Bae SC. Runx2 is a common target of transforming growth factor beta1 and bone morphogenetic protein 2, and cooperation between runx2 and smad5 induces osteoblast-specific gene expression in the pluripotent mesenchymal precursor cell line c2c12. *Mol Cell Biol* 2000;**20**:8783–8792.
23. Ge Y, Sun Y, Chen J. Igf-ii is regulated by microrna-125b in skeletal myogenesis. *J Cell Biol* 2011;**192**:69–81.
24. Zhang Y, Xie RL, Croce CM, Stein JL, Lian JB, van Wijnen AJ, Stein GS. A program of micrornas controls osteogenic lineage progression by targeting transcription factor runx2. *Proc Natl Acad Sci USA* 2011;**108**:9863–9868.
25. Brennecke J, Stark A, Russell RB, Cohen SM. Principles of microrna-target recognition. *PLoS Biol* 2005;**3**:e85.
26. Sinnaeve PR, Donahue MP, Grass P, Seo D, Vonderscher J, Chibout SD, Kraus WE, Sketch M Jr, Nelson C, Ginsburg GS, Goldschmidt-Clermont PJ, Granger CB. Gene expression patterns in peripheral blood correlate with the extent of coronary artery disease. *PLoS ONE* 2009;**4**:e7037.
27. Liao M, Zou S, Weng J, Hou L, Yang L, Zhao Z, Bao J, Jing Z. A microrna profile comparison between thoracic aortic dissection and normal thoracic aorta indicates the potential role of micrornas in contributing to thoracic aortic dissection pathogenesis. *J Vasc Surg* 2011;**53**:1341–1349 e1343.
28. Khanna A, Muthusamy S, Liang R, Sarojini H, Wang E. Gain of survival signaling by down-regulation of three key mirnas in brain of calorie-restricted mice. *Aging (Albany NY)* 2011;**3**:223–236.
29. Zaina S, Pettersson L, Ahren B, Branen L, Hassan AB, Lindholm M, Mattsson R, Thyberg J, Nilsson J. Insulin-like growth factor ii plays a central role in atherosclerosis in a mouse model. *J Biol Chem*. 2002;**277**:4505–4511.
30. Chen L, Jiang W, Huang J, He BC, Zuo GW, Zhang W, Luo Q, Shi Q, Zhang BQ, Wagner ER, Luo J, Tang M, Wietholt C, Luo X, Bi Y, Su Y, Liu B, Kim SH, He CJ, Hu Y, Shen J, Rastegar F, Huang E, Gao Y, Gao JL, Zhou JZ, Reid RR, Luu HH, Haydon RC, He TC, Deng ZL. Insulin-like growth factor 2 (igf-2) potentiates bmp-9-induced osteogenic differentiation and bone formation. *J Bone Miner Res* 2010;**25**:2447–2459.
31. Hamidouche Z, Fromigue O, Ringe J, Haupl T, Marie PJ. Crosstalks between integrin alpha 5 and igf2/igfbp2 signalling trigger human bone marrow-derived mesenchymal stromal osteogenic differentiation. *BMC Cell Biol* 2010;**11**:44.
32. Kang H, Sung J, Jung HM, Woo KM, Hong SD, Roh S. Insulin-like growth factor 2 promotes osteogenic cell differentiation in the parthenogenetic murine embryonic stem cells. *Tissue Eng Part A* 2012;**18**:331–341.
33. Palermo C, Manduca P, Gazzerro E, Foppiani L, Segat D, Barreca A. Potentiating role of igfbp-2 on igf-ii-stimulated alkaline phosphatase activity in differentiating osteoblasts. *Am J Physiol Endocrinol Metab* 2004;**286**:E648–E657.
34. Bergman D, Halje M, Nordin M, Engstrom W. Insulin-like growth factor 2 in development and disease: a mini-review. *Gerontology* 2013;**59**:240–249.